Electrochemical Exfoliation of Graphene and Formation of its Copolyamide 6/66 Nanocomposites by Wet Phase Inversion and Injection Molding

Daniel Ehjeij, Jordan Kopping, Claus Gabriel, Josef R. Wünsch, Hans-Jörg Himmel, Rasmus R. Schröder, Manfred Wilhelm, Jan Freudenberg, Uwe H. F. Bunz, and Klaus Müllen*

Electrochemically exfoliated graphene (EEG) is compounded with copolyamide 6/66 (PA6/66) to investigate the influence of the carbonaceous filler material on the thermal, rheological, and mechanical properties of the composite. Toward that end, the environmentally friendly electrochemical exfoliation in aqueous solution is further developed to furnish graphene in large quantities. Separating the exfoliation process from the incorporation into the polymer matrix by wet phase inversion (WPI) allowed in-depth characterization of the EEG by scanning electron microscopy (SEM), atomic force microscopy (AFM), and Raman spectroscopy. The crystallinity of copolyamide 6/66-EEG is significantly changed, as revealed by differential scanning calorimetry (DSC). Likewise, the new composite materials exhibit different flow properties, as well as increased mechanical reinforcement with additive concentration. This is proven by dynamic shear rheology and three-point stress tests compared to the neat polymer.

1. Introduction

The present paper has a dual purpose: first, to scale up the electrochemically assisted exfoliation of graphene sheets. This is the key requirement to, second, study the compounding of polyamide 6/66. Graphene plays an important role in electronic[1] and energy storage devices[2] as well as in strengthening composite materials.[3] Methods for large-scale production include mechanical (shear mixing[4] or ball milling[5]) or chemical exfoliation by oxidation of graphite to graphite oxide (GO),[6] Flash Joule heating[7] as well as electrochemical procedures.[8–10,11] Graphite has been treated with strong oxidants,[12,13] followed by thermal expansion and reduction to furnish reduced GO. This method, however, has significant disadvantages such as the use of toxic reagents and the risk of intercalating metal impurities. In contrast, electrochemical exfoliation[14] offers a low-cost, environmentally friendly, and scalable alternative avoiding transition-metal impurities.[10,15a–e,16] Parvez et al.[8] investigated the influence of different sulfate salts to control the quality of electrochemically exfoliated graphene (EEG): Besides sodium and potassium sulfate, ammonium sulfate led to large (up to 44 μm in one dimension) EEG flakes (yields > 85%) with a low number of oxidative defects.[8]

2D carbonaceous nanofillers such as graphene nanoplatelets (GNPs)[17] and graphene oxide (GO)[18,19] endow materials with flame retarding,[20] heat dissipative,[21] sensoric,[22] conductive,[23] and mechanically reinforcing[24] properties. Graphene exhibits high thermal and electrical conductivity[25,26] and pronounced mechanical stress tolerance.[27,28]

D. Ehjeij, K. Müllen
Max Planck Institute for Polymer Research
Ackermannweg 10, 55128 Mainz, Germany
E-mail: muellen@mpip-mainz.mpg.de
D. Ehjeij, J. Freudenberg, U. H. F. Bunz
Organisch-Chemisches Institut
Ruprecht-Karls-Universität Heidelberg
Im Neuenheimer Feld 270, 69120 Heidelberg, Germany

J. Kopping, C. Gabriel, J. R. Wünsch
BASF SE
RAP/ODL – B001, 67056 Ludwigshafen am Rhein, Germany
H.-J. Himmel
Anorganisch-Chemisches Institut
Ruprecht-Karls-Universität Heidelberg
Im Neuenheimer Feld 270, 69120 Heidelberg, Germany
R. R. Schröder
BioQuant
Ruprecht-Karls Universität Heidelberg
69120 Heidelberg, Germany
M. Wilhelm
Institute for Chemical Technology and Polymer Chemistry (ITCP)
Karlsruhe Institute of Technology (KIT)
76131 Karlsruhe, Germany
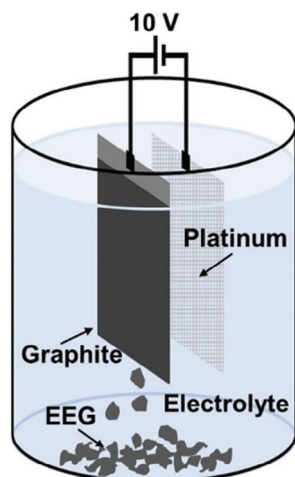J. Freudenberg, U. H. F. Bunz
InnovationLab
69115 Heidelberg, Germany

Figure 1. Electrochemical exfoliation setup: graphite foil parallel to a platinum mesh electrode in a 0.1 M aqueous $(NH_4)_2SO_4$ solution as electrolyte with an operating voltage of 10 V.

While the impact of GO and GNPs on polyamide[29] matrices was extensively studied,[18,30a–f,31,32] that of EEG still remains to be investigated. Here, we present a method for the formation of EEG-reinforced PA6/66 composite materials. We describe the detailed fabrication of low-oxidized large graphene sheets via environmentally friendly[8,33] electrochemical exfoliation, and then proceed to compounding with PA6/66. Combining both processes discloses clear structure-activity relationships together with the thermal, melt rheological, and solid mechanical properties of the polymer composite. Prior to compounding, the exfoliated graphene was characterized via scanning electron microscopy (SEM), atomic force microscopy (AFM), and Raman spectroscopy. The effect of EEG on PA6/66 was investigated by thermogravimetric analysis (TGA), differential scanning calorimetry (DSC), SEM, oscillatory rheology, and three-point stress tests of injection molded bending rods.

2. Results and Discussion

2.1. Graphene Preparation by Electrochemical Exfoliation and Characterization

To scale up the EEG fabrication, (**Figure 1**) the following changes were made from the literature procedures to offer significant improvements of the protocol:[13,67] 1) 2D electrodes were tested instead of wires (see Section S1, Supporting Information) with a platinum mesh (25 cm^2) giving the best results. 2) A graphite foil (25 cm^2 area size) replaced graphite flakes adhering to conductive carbon tape as working electrode. If the foil was too thin (0.13 mm thickness, ≈0.4 g), bending deformations of the foil, induced by the gas evolution, were observed, resulting in contacts with the counter electrode in some cases. A thicker graphite foil (0.5 mm thickness, ≈1.5 g) was dimensionally stable ensuring a uniform distance without short circuits. 3) Instead of polytetrafluoroethylene (0.1 μm pore size), polyvinylidene fluoride filter membranes (0.1 μm pore size) were used for material collection and washing. This significantly sped up the purification process with washing

cycles of only a few minutes. With these optimizations, an exfoliation rate of 750 mg h^{-1} was achieved.

Subsequently, the dry material was suspended in dimethylformamide using mild ultrasound treatment. Usage of an ultrasonic finger gave partially curled flakes (Figures S1 and S2, Supporting Information)[34] which was avoided with a milder, low-intensity ultrasonic bath, resulting in planar flakes. The graphene flakes were stabilized by the solvent for several days without apparent agglomeration. After resting for 2 d to precipitate non-exfoliated particles, the suspension was used for further conversion into composite materials.

The present scale-up approach also improved the morphology of the exfoliated graphene sheets: compared to literature,[10,35] the average layer thickness decreased from 2.2 to 1.8 layers (shifting towards a higher fraction of monolayers) while the number of flakes larger than 10 μm increased (for a detailed analysis via SEM and AFM, see Section S2, Supporting Information). Our EEG was free of defects such as oxygen adducts when compared to other EEG[8,36] (see Raman characterization, Section S2, Supporting Information). All these findings confirm the value of the improved electrochemical exfoliation.

2.2. Reinforcing PA6/66 with EEG

The EEG was embedded into a PA6/66 matrix (**Figure 2**) to investigate the influence of low-content graphene on the composite material. After filtration, the collected EEG paste was suspended and added to a PA6/66 solution (both in formic acid). The mixture was isolated by wet phase inversion (water) to obtain the black PA/G$_x$ masterbatch. The weight fractions of the EEG relative to the composites were between 3.5 and 4.5 wt.% – that is, between 52% and 66% of the original graphite foil were ablated as EEG. The EEG was homogeneously dispersed (SEM images of PA/G$_{4.1}$, **Figure 3A,B**); thereby, larger graphitic particles were absent. To summarize, two simple steps, solvent blending and wet phase inversion, readily provide available masterbatches of PA6/66 with a homogeneous distribution of the EEG filler.

Bending rods of different EEG concentrations from 0 to 2.0 wt.% were then injection molded from the masterbatches into the form of Charpy test bars (64 × 10 × 0.4 mm^3, twin-screw extruder, Figure 3C).

The glass transition and melting temperatures of the composites were only slightly affected by the EEG independent of the filler levels (DSC, **Figure 4A**; and see Section S3, Supporting Information). Crystallinity was influenced more profoundly: In the first heating run, the melting enthalpy of samples with EEG (> 1.0 wt.%) increased from 49% to 57% (see Section S3, Supporting Information). The cooling thermograms of PA/G$_x$ showed only one crystallization peak. The crystallization temperature T_C and the crystallization onset temperature T_{CO} increased by 5 °C and 15 °C (addition 0.1 wt.% EEG), respectively. An elevated plateau was then reached, with T_{CO} again increasing significantly by another 7 °C at 2.0 wt.%. Obviously, EEG serves as a nucleating agent for the thermally more stable α-crystal form:[37] Of the two melting points of polyamide (α-crystal and γ-crystal form)[38] in the second heating TGA cycle, that of the latter one is absent for PA/G$_{2.0}$ (Figure 4C) suggesting that the well-dispersed EEG flakes favor formation of the α-crystal form.[39,40]

ADVANCED
SCIENCE NEWS

www.advancedsciencenews.com

Macro-
molecular
Chemistry and Physics
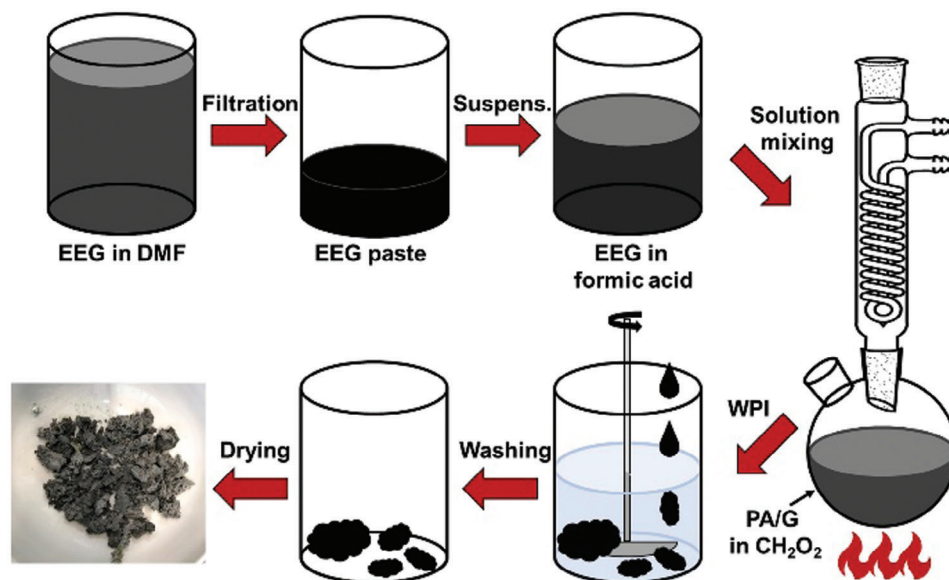
www.mcp-journal.de

Figure 2. Schematic representation of the PA/G_x composite masterbatch production.

Embedding EEG into PA6/66 increases the thermostability of the composites by up to 8 °C (at 0.7 wt.% loading; TGA, Figure S7, Supporting Information), in line with the effect of graphene nanoplatelets as nanofiller in different polyamides.[39,40] It can be said, that the EEG and the PA6/66 matrix interact at the interface, decreasing the mobility of the polymer chains near the interface and increasing the thermal stability of the composite material.

To investigate the homogeneity of the graphene flakes within the polymer matrix and the processability of the PA/G_x composites, oscillatory shear rheology was used to characterize the fundamental flow behavior of the materials (see Section S4, Supporting Information). Figure 4D presents the effect of angular frequency on the elastic shear modulus G′ and viscous shear modulus G″ for neat PA6/66 and nanocomposites of different EEG concentrations, including a multimode Maxwell model (see Section S4, Supporting Information). As expected, G′ and G″ increase with EEG content. At 2.0 wt.% EEG concentration, a flattening of the viscous modulus was observed in the low-frequency range.[41,42] Increasing elastic and viscous shear moduli with elevating graphene concentration in PA6 has been reported.[43] As the graphene ratio increases, the values for G′ approach those of G″ (Figure 4D), which demonstrates the beginning of the formation of a percolation threshold.[32] However, up to 2 wt.%, no transition and therefore no rheological percolation has yet been achieved.[44] The mechanical loss factor tan(δ) as a function of angular frequency is displayed in Figure 4E. Between 0.1 and 1000 rad s^{-1}, the mechanical loss of neat PA6/66 and PA/G_x composites decreases monotonically up to 0.7 wt.% EEG while peak values ≈0.8 rad s^{-1} are observed for the PA/$G_{1.0}$ and PA/$G_{2.0}$ composites. A shift in the peak value of the mechanical loss as a function of angular frequency shows additional energy loss in the form of shear.[45] Figure 4F quantifies the structural viscosity of the composite. Increasing EEG content leads to an increase of the absolute value of the complex viscosity of the composite material, which has been reported.[46] With increasing shear force the viscosity diminishes.[41]

The outstanding mechanical properties of graphene[27] make it a promising filler material. Yet, graphene tends to form agglomerates which may disallow the use of its high intrinsic mechanical properties in composites.[47] All bending rods were analyzed with regard to their mechanical properties in a three-point stress test (see Section S5, Supporting Information). **Figure 5A** shows the results of the measured Young's moduli via a stress-strain experiment as a function of the concentration series. The Young's modulus already increases by 4% with low EEG addition of 0.1 wt.%. Subsequently, a plateau is reached until it again experiences an increase of 13% at 2.0 wt.% of EEG. The bending stress is
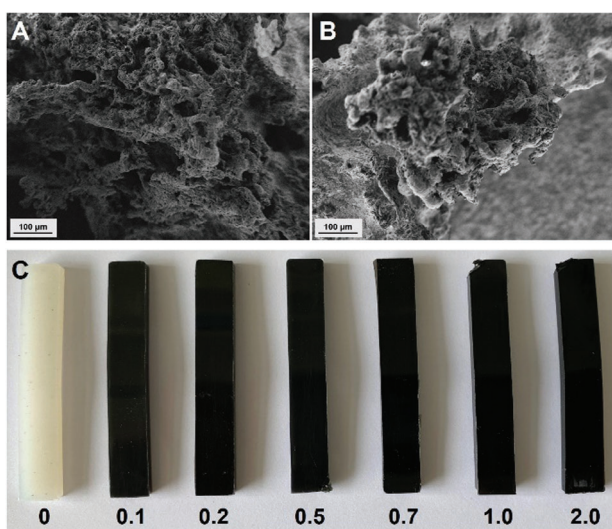

Figure 3. A,B) SEM images of the PA/$G_{4,1}$ composite masterbatch. C) photograph of the bending rods (64 × 10 × 0.4 mm^3) of 0 – 2.0 wt.% EEG content in PA6/66. Samples were taken from the bottom right corner (0.5 wt.% rod) as well as the top left corners (1.0 and 2.0 wt.% rods) for TGA after the mechanical stress tests.
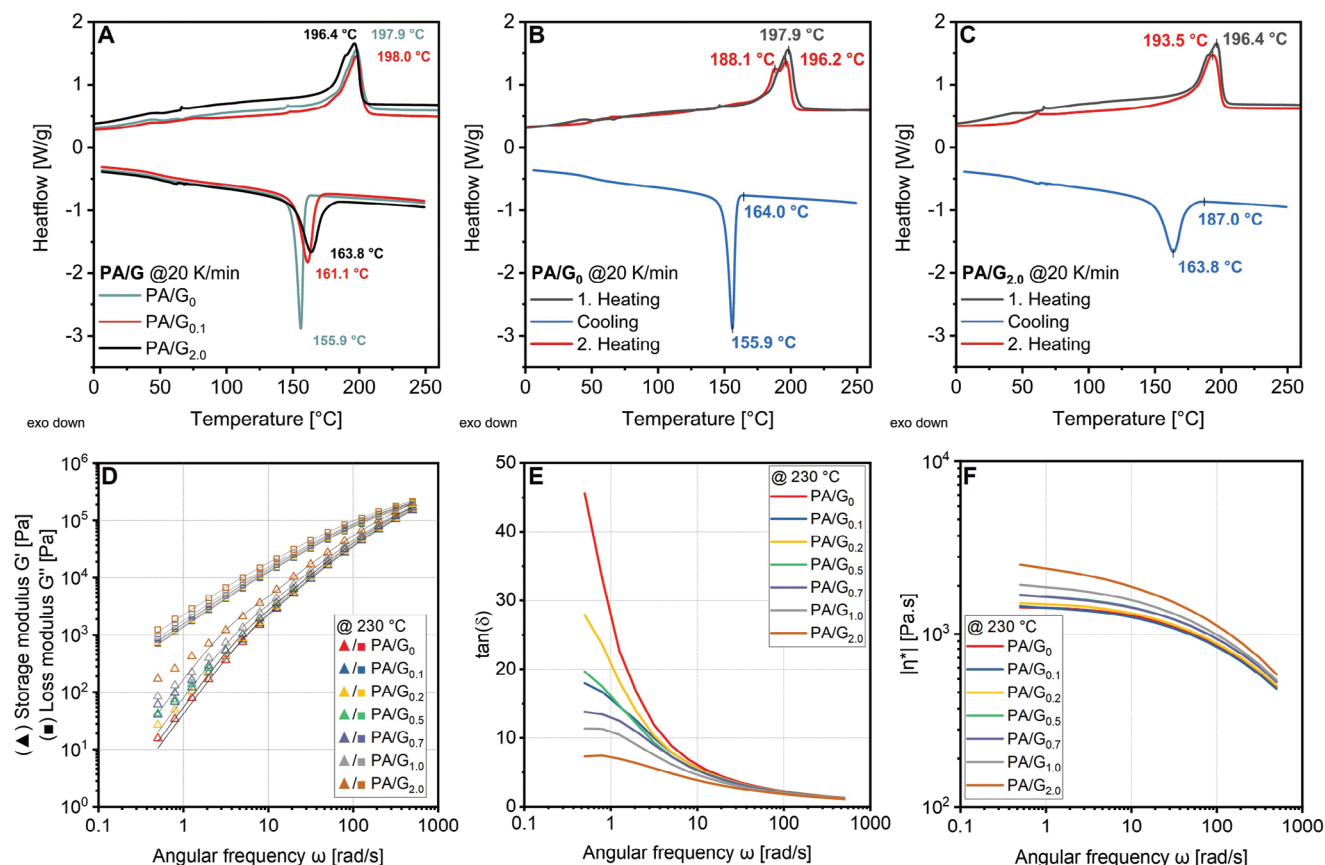
**ADVANCED
SCIENCE NEWS**

www.advancedsciencenews.com

[M]acro-
molecular
Chemistry and Physics

www.mcp-journal.de

Figure 4. A) DSC graph of PA/G$_0$, PA/G$_{0.1}$ and PA/G$_{2.0}$ in a heating-cooling process. DSC graph of B) PA/G$_0$ and C) PA/G$_{2.0}$ in a heating-cooling-heating process up to 270 °C. D) Dynamic viscoelastic response of storage G' and loss moduli G". The Maxwell model (black solid line) is fitted to the experimental results. E) Mechanical loss factor tan(δ) and F) magnitude of complex viscosity of the PA6/66 bending rods of different EEG content as a function of angular frequency at 230 °C.

presented in Figure 5B. An increase in bending modulus can be observed even at low graphene addition. Likewise, a plateau is evident until the bending stress increases again at 2.0 wt.% of EEG filler (see Section S5, Supporting Information). Zhang et al.[48] succeeded in increasing the tensile strength and Young's modulus of PA6 by 66.5% and 88.0%, respectively, by adding 1.0 wt.%

graphene oxide. However, the elongation at break of the composite was significantly lower, which was due to the reduction of intermolecular interactions between the polymers. Yu et al.[49] succeeded in improving the Young's modulus by 29.1% upon embedding 0.5 wt.% exfoliated graphene in a PA6 matrix. Monticelli et al.,[50] on the other hand, observed a significant decrease
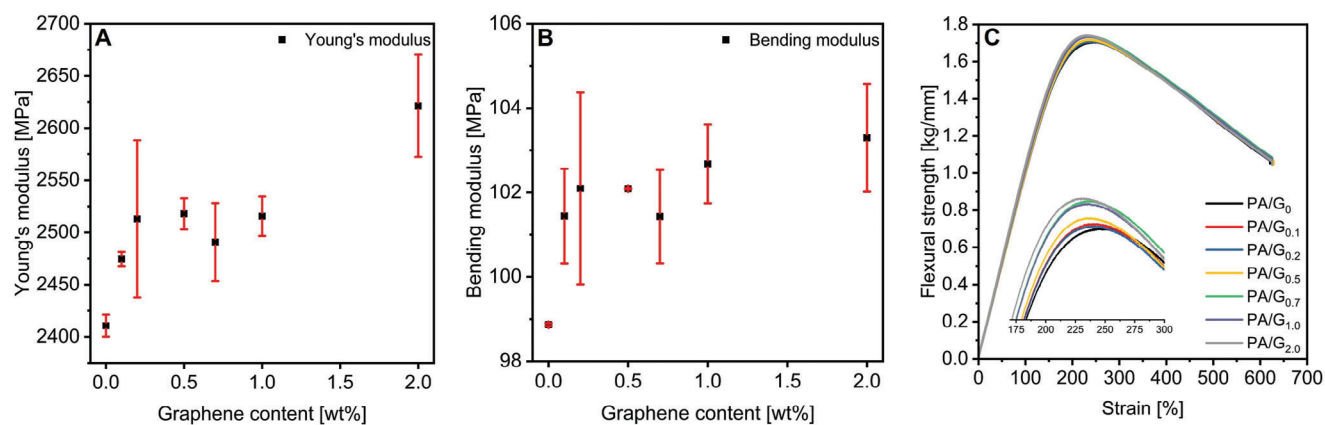

Figure 5. Measured A) Young's modulus, B) bending modulus, C) flexural strength of the bending rods ($64 \times 10 \times 0.4$ mm^3) with different EEG content. Mechanical characteristics were measured with two identical specimens and the results averaged for evaluation.

**ADVANCED
SCIENCE NEWS**

www.advancedsciencenews.com

**M acro-
olecular
Chemistry and Physics**

www.mcp-journal.de

in the modulus of elasticity by adding 0.5 (−45%) or 1.0 wt.% (−36%) exfoliated graphene in PA6, while the elongation at break increased slightly (+1.2% for 0.5 wt.% and +26% for 1.0 wt.%). This was attributed to a plasticizing effect.[51] Due to the improvement in Young's modulus, as well as in bending stress, a reinforcement of the composite material is achieved, while a plasticizing effect of the EEG on the composite material is excluded.

3. Conclusion

An environmentally friendly two-step process for the preparation of copolyamide 6/66/EEG composites has been realized. The protocol starts with electrochemically assisted exfoliation of graphene, followed by wet phase inversion and compounding. The electrochemical exfoliation of graphene can easily be brought to a gram-scale underlining its relevance for further scaling up and industrial purposes. The EEG (up to 66% yield) offers an average size of ≈12 µm and average height of ≈1.8 layers. The choice of electrodes (large area platinum mesh in combination with a thick graphite foil) is of crucial importance yielding graphene flakes larger than 10 µm with a decrease in average layer thickness. 96% are thin-layer graphene with monolayers forming the largest fraction. Raman spectroscopy confirms the high quality of EEG with a low fraction of oxygen adducts. Changing the filtration set-up (PTFE vs PVDF) leads to a rapid isolation of the EEG. Compounds with PA6/66 were fabricated by wet phase inversion. The resulting masterbatches containing up to 4.5 wt.% EEG were then adjusted to the desired concentration ratios using a twin-screw extruder. EEG proves highly suitable for mechanical reinforcement of polyamides: 1) EEG as a nucleation agent stabilizes the more thermally stable α-phase and suppresses other crystal phases with an earlier onset of crystallization of PA6/66. 2) EEG increases thermal degradation temperature of the copolymer by 8 °C and thus improves the thermostability of the polymer due to the well dispersed EEG. 3) The addition of EEG causes an increase in viscosity due to the strong interaction between the PA6/66 matrix and the EEG flakes since the latter restricts the mobility of the PA6/66 strands. Both the Young's modulus (+ 13%) and the bending stress (+ 4%) are enhanced by embedding EEG in the PA6/66 matrix.

To conclude, electrochemical exfoliation appears as an experimentally straightforward and viable procedure to fabricate graphene on a larger scale, while offering an attractive agent for adjusting the filler material due to its low defect density, for example by post-modification.

4. Experimental Section

Apparatus: A power supply (3000B, Powerbox, Sweden) was used as voltage source for the electrochemical exfoliation. SEM images were taken with a field-emission scanning electron microscope (Ultra 55, Carl Zeiss Microscopy, Germany) at 1.5 keV primary electron energy using the SE2 detector for Type II secondary electrons. AFM measurements were conducted using a Bruker Nanoscope MultiMode VIII. Raman spectra were recorded with a Horiba Jobin Yvon T64000 (laser wavelength 514 nm). Mild sonication was realized with a Transsonic T 490 DH by Elma. A Heidolph RZR 2052 propeller stirrer was employed to precipitate the composite masterbatches. TGA samples and masterbatches were dried in a Vacutherm vacuum oven by Heraeus Instruments. Compounding of the mas-

terbatches was carried out with a Xplore micro compounder MC 15 (laboratory twin-screw extruder, screw length 336 mm, mixing length 172 mm, diameter 22 – 9 mm) with a rotational speed of 80 rpm at 230 °C. The material (masterbatch and neat copolyamide 6/66) was added into the extruder within 1 min and then compounded for another 3 min before being injected at 230 °C into the mold preheated at 120 °C (pressure was 16 bar during injection for 5 s and then maintained at 14 bar for further 5 s). TGA was measured using a Mettler Toledo TGA/DSC (30–800 °C, heating rate 10 K min^{-1} under nitrogen atmosphere). DSC measurements were performed with a TA-Instruments DSC Q2000 (25 – 270 °C, heating rate 20 K min^{-1}) device. The apparent crystalline content of the composites was determined using a value of 151 J g^{-1} for the heat of fusion for a theoretically 100% crystalline PA6/66.[52] Dynamic shear rheology measurements were carried out with the oscillatory rheometer DHR-1 by TA-Instruments with 25 mm diameter parallel-plate fixture (1 mm gap between the parallel plates). The measurements were performed at 230 °C. Frequency sweep tests were conducted in a range of 500 – 0.5 rad s^{-1} at a strain of 1.0%. All specimens ($64 \times 10 \times 0.4$ mm^3) were dried in a vacuum oven at 50 °C for at least 72 h. Mechanical stress tests were performed at room temperature on a three-point setup (Texture Analyzer TA-HD by Stable Micro Systems, force resolution 0.1 g, support distance 64 mm, diameter of the supporting rolls 10 mm, traverse speed of the Young modulus 0.1 mm s^{-1}, maximum strain for determining the Young modulus 0.25%, traverse speed of determination stability 0.3 mm s^{-1}, crosshead travel 25 mm) with injection molded bending rods ($64 \times 10 \times 0.4$ mm^3) with different EEG content.

Electrochemical Exfoliation of Graphite: Graphite exfoliation was carried out in a two-electrode system adapting a procedure published by Parvez et al.[8] In a 1 L beaker filled with 900 mL of a 0.1 molar aqueous ammonium sulfate ((NH_4)$_2$SO$_4$, Sigma-Aldrich) electrolyte solution, a platinum mesh electrode (50×50 mm^2 size, wire diameter 0.06 mm) and a graphite foil (Alfa Aesar, 0.5 mm thick, 99.8% metals basis, 50×50 mm^2, ≈1.4 g) as counter electrode were placed in parallel at a fixed distance of 2 cm. When a static potential of 10 V was applied, the graphite electrode was ablated, causing exfoliated graphite material to accumulate at the surface of the electrolyte solution and as a sediment (≈1 h). The exfoliated graphitic material was allowed to settle for 1 h before most of the electrolyte solution was decanted off (ca. 90%). The exfoliated material was collected by filtration (PVDF; 0.1 µm pore size, 47 mm diameter) and washed thoroughly with DI water and ethanol respectively. Using mild ultrasound (20%, 60 min, rt), the wet material was suspended in 0.5 L DMF, upon which individual flakes were split off from the graphitic material and stabilized by the solvent due to lack of reaggregation of the graphene flakes.[53] The EEG suspension (52–66% with respect to the initial graphite foil) was allowed to rest for 48 h to settle down un-exfoliated graphitic material and larger fragments.

Composite Masterbatch Fabrication: The PA6/66/EEG (PA/G$_x$ where x indicates the mass fraction of EEG) composites were synthesized adapting a procedure of Scaffaro.[54] For PA/G$_x$ composite masterbatch fabrication, the top 90% of the EEG suspension was filtered (PTFE, 0.5 µm pore size, 47 cm diameter), yielding a graphene paste. This paste was suspended in 150 mL of formic acid (98+% purity, Acros Organics) using mild ultrasonication (40%, 20 min, rt). The suspension was then added to a 60 °C solution of 20 g of PA6/66 (Ultramid C33 01 provided by BASF SE, degree of crystallinity 0.36–0.56, melting temperature 196 °C) in 200 mL of formic acid (10 mL g^{-1}) and stirred for 1 h. The resulting dissolved PA/G$_x$ mixture was transferred to a beaker filled with water and equipped with a propeller stirrer and subsequently precipitated by WPI in 1 L DI water. As the formic acid migrated into the aqueous phase, the sponge-like PA/G$_x$ masterbatch precipitated and was collected by filtration. This solid was found to prevent a stirring bar from rotating sufficiently, so the use of a propeller stirrer proved instrumental in fabricating the composite masterbatches. The resulting composite material was washed with DI water until a neutral pH was achieved. The PA/G composite masterbatch was finally dried at 80 °C in a vacuum oven for 72 h. Twin-screw extrusion was used to produce composites (bending rods and samples for TGA/DSC and rheology) of concentrations ranging from 0 to 2 wt.% EEG content from the masterbatches.

Supporting Information

Supporting Information is available from the Wiley Online Library or from the author.

Acknowledgements

Conflict of Interest

The authors declare no conflict of interest.

Data Availability Statement

The data that support the findings of this study are available in the supplementary material of this article.

Keywords

[1] a) N. Yogeswaran, E. S. Hosseini, R. Dahiya, *ACS Appl. Mater. Interfaces* **2020**, *12*, 54035; b) S. Parui, M. Ribeiro, A. Atxabal, R. Llopis, F. Casanova, L. E. Hueso, *Nanoscale* **2017**, *9*, 10178;

[2] a) Z.-S. Wu, K. Parvez, X. Feng, K. Müllen, *Nat. Commun.* **2013**, *4*, 2487; b) H. Huang, F. Zhou, P. Lu, X. Li, P. Das, X. Feng, K. Müllen, Z.-S. Wu, *Energy Storage Mater.* **2020**, *27*, 396; c) C. Xu, B. Xu, Y. Gu, Z. Xiong, J. Sun, X. S. Zhao, *Energy Environ. Sci.* **2013**, *6*, 1388;

[3] a) K. Parvez, S. B. Yang, Y. Hernandez, A. Winter, A. Turchanin, X. L. Feng, K. Mullen, *ACS Nano* **2012**, *6*, 9541; b) Y. Ren, Y. Zhang, H. Guo, R. Lv, S.-L. Bai, *Composites, Part A* **2019**, *126*, 105578; c) A. R. Vázquez, C. Neumann, M. Borrelli, H. Shi, M. Kluge, W. Abdel-Haq, M. R. Lohe, C. Gröber, A. Röpert, A. Turchanin, *Nanoscale* **2021**, *13*, 15859;

[4] K. R. Paton, E. Varrla, C. Backes, R. J. Smith, U. Khan, A. O'Neill, C. Boland, M. Lotya, O. M. Istrate, P. King, T. Higgins, S. Barwich, P. May, P. Puczkarski, I. Ahmed, M. Moebius, H. Pettersson, E. Long, J. Coelho, S. E. O'Brien, E. K. McGuire, B. M. Sanchez, G. S. Duesberg, N. McEvoy, T. J. Pennycook, C. Downing, A. Crossley, V. Nicolosi, J. N. Coleman, *Nat. Mater.* **2014**, *13*, 624.

[5] I.-Y. Jeon, Y.-R. Shin, G.-J. Sohn, H.-J. Choi, S.-Y. Bae, J. Mahmood, S.-M. Jung, J.-M. Seo, M.-J. Kim, D. Wook Chang, L. Dai, J.-B. Baek, *Proc. Natl. Acad. Sci. USA* **2012**, *109*, 5588.

[6] H. L. Poh, F. Šaněk, A. Ambrosi, G. Zhao, Z. Sofer, M. Pumera, *Nanoscale* **2012**, *4*, 3515.

[7] D. X. Luong, K. V. Bets, W. A. Algozeeb, M. G. Stanford, C. Kittrell, W. Chen, R. V. Salvatierra, M. Ren, E. A. McHugh, P. A. Advincula, Z. Wang, M. Bhatt, H. Guo, V. Mancevski, R. Shahsavari, B. I. Yakobson, J. M. Tour, *Nature* **2020**, *577*, 647.

[8] K. Parvez, Z.-S. Wu, R. Li, X. Liu, R. Graf, X. Feng, K. Müllen, *J. Am. Chem. Soc.* **2014**, *136*, 6083.

[9] K. Parvez, R. Li, S. R. Puniredd, Y. Hernandez, F. Hinkel, S. Wang, X. Feng, K. Müllen, *ACS Nano* **2013**, *7*, 3598.

[10] K. Parvez, S. Yang, X. Feng, K. Müllen, *Synth. Met.* **2015**, *210*, 123.

[11] a) P. Yu, S. E. Lowe, G. P. Simon, Y. L. Zhong, *Curr. Opin. Colloid Interface Sci.* **2015**, *20*, 329; b) J. Lu, J.-X. Yang, J. Wang, A. Lim, S. Wang, K. P. Loh, *ACS Nano* **2009**, *3*, 2367; c) P. C. Shi, J. P. Guo, X. Liang, S. Cheng, H. Zheng, Y. Wang, C. H. Chen, H. F. Xiang, *Carbon* **2018**, *126*, 507;

[12] G. Allaedini, E. Mahmoudi, P. Aminayi, S. M. Tasirin, A. W. Mohammad, *Synth. Met.* **2016**, *220*, 72.

[13] H. Yu, B. Zhang, C. Bulin, R. Li, R. Xing, *Sci. Rep.* **2016**, *6*, 36143.

[14] M. Zhao, C. Casiraghi, K. Parvez, *Chem. Soc. Rev.* **2024**, *53*, 3036.

[15] a) K. Ghosh, S. Ng, C. Iffelsberger, M. Pumera, *Chem.-Eur. J.* **2020**, *26*, 15746; b) A. Ambrosi, C. K. Chua, B. Khezri, Z. Sofer, R. D. Webster, M. Pumera, *Proc. Natl. Acad. Sci. USA* **2012**, *109*, 12899; c) F. Kang, Y. Leng, T.-Y. Zhang, *J. Phys. Chem. Solids* **1996**, *57*, 889; d) P. K. MK, S. Shanthini, C. Srivastava, *RSC Adv.* **2015**, *5*, 53865; e) S. Yang, M. R. Lohe, K. Müllen, X. Feng, *Adv. Mater.* **2016**, *28*, 6213;

[16] C.-Y. Su, A.-Y. Lu, Y. Xu, F.-R. Chen, A. N. Khlobystov, L.-J. Li, *ACS Nano* **2011**, *5*, 2332.

[17] a) H. S. Kim, H. S. Bae, J. Yu, S. Y. Kim, *Sci. Rep.* **2016**, *6*, 26825; b) S. Ming-Yuan, C. Tung-Yu, H. Tsung-Han, L. Yi-Luen, C. Chin-Lung, Y. Hsiharng, Y. Ming-Chuen, *J. Nanomater.* **2013**, *2013*, 565401. c) X. Luo, G. Yang, D. W. Schubert, *Adv. Compos. Hybrid Mater.* **2022**, *5*, 250;

[18] X. Fu, C. Yao, G. Yang, *RSC Adv.* **2015**, *5*, 61688.

[19] H. Feng, Y. Li, J. Li, *RSC Adv.* **2012**, *2*, 6988.

[20] a) N. F. Attia, S. E. A. Elashery, A. M. Zakria, A. S. Eltaweil, H. Oh, *Mater. Sci. Eng. B* **2021**, *274*, 115460; b) D. A. Pethsangave, R. V. Khose, P. H. Wadekar, S. Some, *ACS Sustainable Chem. Eng.* **2019**, *7*, 11745;

[21] a) S. Cui, F. Jiang, N. Song, L. Shi, P. Ding, *ACS Appl. Mater. Interfaces* **2019**, *11*, 30352; b) C. B. Kim, J. Lee, J. Cho, M. Goh, *Carbon* **2018**, *139*, 386;

[22] a) X. Zhang, D. Xiang, Y. Wu, E. Harkin-Jones, J. Shen, Y. Ye, W. Tan, J. Wang, P. Wang, C. Zhao, Y. Li, *Composites, Part A* **2021**, *151*, 106665; b) S. Han, Q. Meng, A. Chand, S. Wang, X. Li, H. Kang, T. Liu, *Polym. Test.* **2019**, *80*, 106106; c) W. Yuan, L. Huang, Q. Zhou, G. Shi, *ACS Appl. Mater. Interfaces* **2014**, *6*, 17003;

[23] a) G. Eda, M. Chhowalla, *Nano Lett.* **2009**, *9*, 814; b) Q. Wu, Y. Xu, Z. Yao, A. Liu, G. Shi, *ACS Nano* **2010**, *4*, 1963.

[24] a) A. Kumar, K. Sharma, A. R. Dixit, *Carbon Lett.* **2021**, *31*, 149; b) S. Han, Q. Meng, Z. Qiu, A. Osman, R. Cai, Y. Yu, T. Liu, S. Araby, *Polymer* **2019**, *184*, 121884; c) H. Gao, J. Xu, S. Liu, Z. Song, M. Zhou, S. Liu, F. Li, F. Li, X. Wang, Z. Wang, Q. Zhang, *J. Colloid Interface Sci.* **2021**, *597*, 393; d) S. Chatterjee, J. W. Wang, W. S. Kuo, N. H. Tai, C. Salzmann, W. L. Li, R. Hollertz, F. A. Nüesch, B. T. T. Chu, *Chem. Phys. Lett.* **2012**, *531*, 6;

[25] a) A. C. Neto, F. Guinea, N. Peres, K. S. Novoselov, A. K. Geim, *Rev. Mod. Phys.* **2009**, *81*, 109; b) K. I. Bolotin, K. J. Sikes, Z. Jiang, M. Klima, G. Fudenberg, J. Hone, P. Kim, H. L. Stormer, *Solid State Commun.* **2008**, *146*, 351;

[26] A. A. Balandin, S. Ghosh, W. Bao, I. Calizo, D. Teweldebrhan, F. Miao, C. N. Lau, *Nano Lett.* **2008**, *8*, 902.

[27] C. Lee, X. Wei, J. W. Kysar, J. Hone, *Science* **2008**, *321*, 385.

[28] a) L. Gomez De Arco, Y. Zhang, C. W. Schlenker, K. Ryu, M. E. Thompson, C. Zhou, *ACS Nano* **2010**, *4*, 2865; b) D. Akinwande, C. J. Brennan, J. S. Bunch, P. Egberts, J. R. Felts, H. Gao, R. Huang, J.-S. Kim, T. Li, Y. Li, K. M. Liechti, N. Lu, H. S. Park, E. J. Reed, P. Wang, B. I. Yakobson, T. Zhang, Y.-W. Zhang, Y. Zhou, Y. Zhu, *Extreme Mech. Lett.* **2017**, *13*, 42;

[29] a) M. Pervaiz, M. Faruq, M. Jawaid, M. Sain, *Curr. Org. Synth.* **2017**, *14*, 146; b) M. Biron, *Thermoplastics and Thermoplastic Composites*, 2nd ed., William Andrew, Norwich, NY **2012**; c) H. Domininghaus, P. Elsner, P. Eyerer, T. Hirth, *Kunststoffe Eigenschaften und Anwendungen*, Springer, Berlin **2008**;

[30] a) P. Ding, S. Su, N. Song, S. Tang, Y. Liu, L. Shi, *Carbon* **2014**, *66*, 576; b) D. Verma, P. C. Gope, A. Shandilya, A. Gupta, *Trans. Indian Inst. Met.* **2014**, *67*, 803; c) D. Zheng, G. Tang, H.-B. Zhang, Z.-Z. Yu, F. Yavari, N. Koratkar, S.-H. Lim, M.-W. Lee, *Compos. Sci. Technol.* **2012**, *72*, 284; d) E. Karatas, O. Gul, N. G. Karsli, T. Yilmaz, *Composites, Part B* **2019**, *163*, 730; e) X. Sun, C. Huang, L. Wang, L. Liang, Y. Cheng, W. Fei, Y. Li, *Adv. Mater.* **2021**, *33*, 2001105; f) J. Vasiljević, A. Demšar, M. Leskovšek, B. Simončič, N. Čelan Korošin, I. Jerman, M. Šobak, G. Žitko, N. van de Velde, M. Čolović, *Polymers* **2020**, *12*, 1787;

[31] X. Zhang, X. Fan, H. Li, C. Yan, *J. Mater. Chem.* **2012**, *22*, 24081.

[32] K. P. M. Lee, M. Brandt, R. Shanks, F. Daver, *Polymers* **2020**, *12*, 2014.

[33] J. Liu, H. Yang, S. G. Zhen, C. K. Poh, A. Chaurasia, J. Luo, X. Wu, E. K. L. Yeow, N. G. Sahoo, J. Lin, *RSC Adv.* **2013**, *3*, 11745.

[34] M. V. Savoskin, V. N. Mochalin, A. P. Yaroshenko, N. I. Lazareva, T. E. Konstantinova, I. V. Barsukov, I. G. Prokofiev, *Carbon* **2007**, *45*, 2797.

[35] S. Yang, A. G. Ricciardulli, S. Liu, R. Dong, M. R. Lohe, A. Becker, M. A. Squillaci, P. Samorì, K. Müllen, X. Feng, *Angew. Chem., Int. Ed.* **2017**, *56*, 6669.

[36] S. Yang, S. Brüller, Z.-S. Wu, Z. Liu, K. Parvez, R. Dong, F. Richard, P. Samorì, X. Feng, K. Müllen, *J. Am. Chem. Soc.* **2015**, *137*, 13927.

[37] M. Liu, Q. Zhao, Y. Wang, C. Zhang, Z. Mo, S. Cao, *Polymer* **2003**, *44*, 2537.

[38] M. Kyotani, S. Mitsuhashi, *J. Polym. Sci. A* **1972**, *10*, 1497.

[39] M. I. Shueb, M. E. Abd Manaf, M. Mohamed, N. Mohamad, J. Abd Razak, N. A. Sani, K. N. K. Umar, *J. Adv. Res. Fluid Mech.* **2022**, *89*, 13.

[40] D. Dixon, P. Lemonine, J. Hamilton, G. Lubarsky, E. Archer, *J. Thermoplast. Compos. Mater.* **2015**, *28*, 372.

[41] J. Canales, M. Fernández, J. J. Peña, M. E. Muñoz, A. Santamaría, *Polym. Eng. Sci.* **2015**, *55*, 1142.

[42] D. Xu, Z. Wang, *Polymer* **2008**, *49*, 330.

[43] B. Mayoral, E. Harkin-Jones, P. N. Khanam, M. A. AlMaadeed, M. Ouederni, A. R. Hamilton, D. Sun, *RSC Adv.* **2015**, *5*, 52395.

[44] J. Canales, M. Fernández, J. J. Peña, M. E. Muñoz, A. Santamaría, *Polym. Eng. Sci.* **2015**, *55*, 1142.

[45] X. Chen, S. Wei, A. Yadav, R. Patil, J. Zhu, R. Ximenes, L. Sun, Z. Guo, *Macromol. Mater. Eng.* **2011**, *296*, 434.

[46] a) R. Bouhfid, F. Z. Arrakhiz, A. Qaiss, *Polym. Compos.* **2016**, *37*, 998; b) E. Cakal Sarac, L. Haghighi Poudeh, I. Berktas, B. Saner Okan, *J. Appl. Polym. Sci.* **2021**, *138*, 49972;

[47] I. A. Kinloch, J. Suhr, J. Lou, R. J. Young, P. M. Ajayan, *Science* **2018**, *362*, 547.

[48] Q. Zhang, F. Fang, X. Zhao, Y. Li, M. Zhu, D. Chen, *J. Phys. Chem. B* **2008**, *112*, 12606.

[49] X. Yu, X. Dong, Z. Song, J. Gui, *Plast. Rubber Compos.* **2020**, *49*, 281.

[50] O. Monticelli, S. Bocchini, A. Frache, E. S. Cozza, O. Cavalleri, L. Prati, *J. Nanomater.* **2012**, *2012*, 938962.

[51] A. Sanz, M. Ruppel, J. F. Douglas, J. T. Cabral, *J. Phys.: Condens. Matter.* **2008**, *20*, 104209.

[52] L. I. Castelan-Velazco, J. Mendez-Nonell, S. Sanchez-Valdes, L. F. Ramos-deValle, *Polym. Bull.* **2009**, *62*, 99.

[53] E. A. Trusova, I. V. Klimenko, A. M. Afzal, A. N. Shchegolikhin, L. V. Jurina, *New J. Chem.* **2021**, *45*, 10448.

[54] R. Scaffaro, A. Maio, *Composites, Part B* **2019**, *165*, 55.

[55] S. Yang, A. G. Ricciardulli, S. Liu, R. Dong, M. R. Lohe, A. Becker, M. A. Squillaci, P. Samorì, K. Müllen, X. Feng, *Angew. Chem.* **2017**, *129*, 6770.

[56] K. S. Novoselov, D. Jiang, F. Schedin, T. J. Booth, V. V. Khotkevich, S. V. Morozov, A. K. Geim, *Proc. Natl. Acad. Sci. USA* **2005**, *102*, 10451.

[57] A. C. Ferrari, J. C. Meyer, V. Scardaci, C. Casiraghi, M. Lazzeri, F. Mauri, S. Piscanec, D. Jiang, K. S. Novoselov, S. Roth, *Phys. Rev. Lett.* **2006**, *97*, 187401.

[58] B. Krauss, T. Lohmann, D.-H. Chae, M. Haluska, K. von Klitzing, J. H. Smet, *Phys. Rev. B* **2009**, *79*, 165428.

[59] F. Zhang, X. Peng, W. Yan, Z. Peng, Y. Shen, *J. Polym. Sci., Part B: Polym. Phys.* **2011**, *49*, 1381.

[60] M. Baibarac, P. Gomez-Romero, M. Lira-Cantu, N. Casañ-Pastor, N. Mestres, S. Lefrant, *Eur. Polym. J.* **2006**, *42*, 2302.

[61] J. Zhang, Z. Qiu, *Ind. Eng. Chem. Res.* **2011**, *50*, 13885.

[62] K. P. M. Lee, M. Czajka, R. Shanks, F. Daver, *J. Appl. Polym. Sci.* **2020**, *137*, 48630.

[63] L. Zhou, H. Liu, X. Zhang, *J. Mater. Sci.* **2015**, *50*, 2797.

[64] a) B. D. S. M. Da Cruz, L. G. P. Tienne, F. F. Gondim, L. Da Silva Candido, E. G. Chaves, M. F. V. Marques, F. S. Da Luz, S. N. Monteiro, *J. Mater. Res. Technol.* **2022**, *18*, 1842; b) J. Sanes, C. Sánchez, R. Pamies, M.-D. Avilés, M.-D. Bermúdez, *Materials* **2020**, *13*, 549;

[65] S. Gaikwad, J. S. Tate, N. Theodoropoulou, J. H. Koo, *J. Compos. Mater.* **2012**, *47*, 2973.

[66] a) S. Chen, Q. Wu, C. Mishra, J. Kang, H. Zhang, K. Cho, W. Cai, A. A. Balandin, R. S. Ruoff, *Nat. Mater.* **2012**, *11*, 203; b) S. Chen, A. L. Moore, W. Cai, J. W. Suk, J. An, C. Mishra, C. Amos, C. W. Magnuson, J. Kang, L. Shi, R. S. Ruoff, *ACS Nano* **2011**, *5*, 321;

[67] a) Y. Wang, H. F. Zhan, Y. Xiang, C. Yang, C. M. Wang, Y. Y. Zhang, *J. Phys. Chem. C* **2015**, *119*, 12731; b) Y. Wang, C. Yang, Y.-W. Mai, Y. Zhang, *Carbon* **2016**, *102*, 311;

[68] C. K. Georgantopoulos, M. K. Esfahani, C. Botha, M. A. Pollard, I. F. C. Naue, A. Causa, R. Kádár, M. Wilhelm, *Phys. Fluids* **2021**, *33*, 093108.

[69] W. Xue-Bang, X. Qiao-Ling, S. Shu-Ying, S. Jia-Peng, L. Chang-Song, Z. Zhen-Gang, *Chin. Phys. Lett.* **2008**, *25*, 1388.

[70] D. I. Bower, *An Introduction to Polymer Physics*, Cambridge University Press, Cambridge **2003**.

[71] R. Scaffaro, A. Maio, *Polymers* **2019**, *11*, 857.

[72] N. I. Kovtyukhova, P. J. Ollivier, B. R. Martin, T. E. Mallouk, S. A. Chizhik, E. V. Buzaneva, A. D. Gorchinskiy, *Chem. Mater.* **1999**, *11*, 771.